SEISMIC DISTANCE-AMPLITUDE RELATIONS FOR SHORT PERIOD P, PDIFF', PP AND COMPRESSIONAL CORE PHASES FOR DELTA LESS THAN 90 DEGREES

E. I. Sweetser, et al

Teledyne Geotech

Prepared for:

Defense Advanced Research Projects Agency

5 November 1973

AD 774 916

SDAC-TR-73-6

SEISMIC DISTANCE-AMPLITUDE RELATIONS FOR SHORT PERIOD P, P dif, PP AND COMPRESSIONAL CORE PHASES FOR $\Delta > 90°$

E. I. SWEETSER, R. A. BLANDFORD

Seismic Data Analysis Center

Teledyne Geotech, 314 Montgomery Street, Alexandria, Virginia 22314

Sponsored By

The Defense Advanced Research Projects Agency

Nuclear Monitoring Research Office

1400 Wilson Boulevard, Arlington, Virginia 22209

ARPA Order No. 1620

Monitored By

VELA Seismological Center

312 Montgomery Street, Alexandria, Virginia 22314

Unclassified

SECURITY CLASSIFICATION OF THIS PAGE (When Data Entered)

REPORT DOCUMENTATION PAGE		READ INSTRUCTIONS BEFORE COMPLETING FORM
1. REPORT NUMBER SDAC-TR-73-9	2. GOVT ACCESSION NO.	3. RECIPIENT'S CATALOG NUMBER
4. TITLE (and Subtitle) SEISMIC DISTANCE-AMPLITUDE RELATIONS FOR SHORT PERIOD P, P_{diff}, PP AND COMPRESSIONAL CORE PHASES FOR $\Delta \geq 90°$		5. TYPE OF REPORT & PERIOD COVERED Technical 6. PERFORMING ORG. REPORT NUMBER
7. AUTHOR(s) Sweetser, E. I., Blandford, R. R.		8. CONTRACT OR GRANT NUMBER(s) F08606-74-C-0006
9. PERFORMING ORGANIZATION NAME AND ADDRESS Teledyne Geotech 314 Montgomery Street Alexandria, Virginia 22314		10. PROGRAM ELEMENT, PROJECT, TASK AREA & WORK UNIT NUMBERS
11. CONTROLLING OFFICE NAME AND ADDRESS Defense Advanced Research Projects Agency Nuclear Monitoring Research Office 1400 Wilson Blvd. Arlington, Va. 22209		12. REPORT DATE 5 Nov 1973 13. NUMBER OF PAGES 49
14. MONITORING AGENCY NAME & ADDRESS(if different from Controlling Office) VELA Seismological Center 312 Montgomery Street Alexandria, Virginia 22314		15. SECURITY CLASS. (of this report) 15a. DECLASSIFICATION DOWNGRADING SCHEDULE

16. DISTRIBUTION STATEMENT (of this Report)

APPROVED FOR PUBLIC RELEASE; DISTRIBUTION UNLIMITED.

17. DISTRIBUTION STATEMENT (of the abstract entered in Block 20, if different from Report)

18. SUPPLEMENTARY NOTES

19. KEY WORDS (Continue on reverse side if necessary and identify by block number)

Seismology
Amplitude-Distance
PKP
Core Phases
PP
Distance-Amplitude
P

20. ABSTRACT (Continue on reverse side if necessary and identify by block number)

Measurements of $\log_{10}(A/T)$ reported by the International Seismic Centre, the Vela Observatories, and the Long-Range Seismic Measurements Program are used to define an amplitude-distance curve for the maximum amplitude in the first few seconds of motion for the distance range $\Delta > 90°$. In general terms, the corresponding phases are P, P_{diff}, and PKIKP. Some information is also obtained, however, for the phases PP and PKP_2.

DD FORM 1 JAN 73 1473 EDITION OF 1 NOV 65 IS OBSOLETE

Unclassified

SECURITY CLASSIFICATION OF THIS PAGE (When Data Entered)

SEISMIC DISTANCE-AMPLITUDE RELATIONS FOR SHORT PERIOD P, P_{diff}, PP AND COMPRESSIONAL CORE PHASES FOR $\Delta > 90°$

Seismic Data Analysis Center Report No.: SDAC-TR-73-9

AFTAC Project No.:	VELA VT/4709
Project Title:	Seismic Data Analysis Center
ARPA Order No.:	1620
ARPA Program Code No.:	3F10
Name of Contractor:	TELEDYNE GEOTECH
Contract No.:	F08606-74-C-0006
Date of Contract:	01 July 1973
Amount of Contract:	$2,152,172
Contract Expiration Date:	30 June 1974
Project Manager:	Robert G. Van Nostrand (703) 836-3882

P. O. Box 334, Alexandria, Virginia 22314

APPROVED FOR PUBLIC RELEASE; DISTRIBUTION UNLIMITED.

ABSTRACT

Measurements of $\log_{10}(A/T)$ reported by the International Seismic Centre, the Vela Observatories, and the Long-Range Seismic Measurements Program are used to define an amplitude-distance curve for the maximum amplitude in the first few seconds of motion for the distance range $\Delta > 90°$. In general terms, the corresponding phases are P, P_{diff}, and PKIKP. Some information is also obtained, however, for the phases PP and PKP_2.

TABLE OF CONTENTS

LIST OF FIGURES

LIST OF FIGURES (Cont'd.)

LIST OF TABLES

INTRODUCTION

Gutenberg and Richter (1956) compiled distance-amplitude relations for short-period earthquake P and S phases in the distance interval $0° < \Delta < 110°$ and for PP in the distance interval $0° < \Delta < 180°$ (see also Richter, 1958), for these data). While many workers subsequently published modifications to Gutenberg's curves for regional distances, Veith and Clawson (1972), using explosion data, were the first to propose a new curve for P over the entire teleseismic range, $0° < \Delta < 100°$.

Denson (1952) produced some PKP amplitudes, but the data were rather sparse, restricted to a few stations, and from early instrumentation with poorly defined characteristics. (See Figures 1 and 2 and the accompanying discussion in the text for definitions of the various phases.) After the introduction of the WWSSN instrumentation several more studies were forthcoming. Subiza and Båth (1964) concentrated on the distance range 120°-140° in examining the precursors to PKIKP. They reported about 100 PKIKP amplitudes, but the events used were pre-1962, for which reported m_b values tend to be unreliable. Thus we could not feel justified in using their data to determine an absolute distance-amplitude scale without a careful restudy of the m_b values for their events. Subiza and Båth did not, of course, intend that their amplitude data be used for such a purpose.

Ergin (1967) reported amplitudes for a few large earthquakes, but not enough to make a significant contribution to a distance-amplitude study.

Shurbet (1967) performed a comprehensive study, personally reading original records, of PKP amplitude versus distance for the range 110°-180°. For each event, he used the amplitude of the event at a station near 125° to normalize all the observations for that event. He found that it was difficult in the caustic zone to distinguish the different phases, and so generally speaking for this distance range he simply plotted the largest amplitude seen. This is the approach which we are forced to take in our use of data from the Bulletin of the International Seismological Centre (ISC); thus his plots form a valuable check on our results. Outside the caustic zone Shurbet determined an average B factor independent of distance. We shall see that this is a considerable oversimplification, especially near the shadow zone.

Engdahl (1968) reported approximately 70 PKP amplitudes together with a comparable number of PKKP and related amplitudes from two earthquakes.

Shahidi (1968) measured maximum values of the PKP group from 25 shallow 1963 earthquakes in the S. W. Pacific as recorded at 6 stations in Sweden. He obtained a total of about 150 A/T values for the distance range $133° \leq \Delta < 153°$. Variable instrumentation and poor NOAA m_b values make this data difficult to use for our purposes.

Ruprechtova (1972) presented observed amplitude ratios between PKIKP, PKHKP, and PKP_2 from 144° to 154° using approximately 100 observations for each phase. As an overall average the ratios were PKHKP/PKIKP $\simeq$ 5 for $145° < \Delta < 151°$; and $PKP_2/PKIKP_2 \simeq 4$ for $145° < \Delta < 154°$. These results are of substantial use in interpreting the ISC data, although it must be kept in mind that perhaps 10% of the values for these ratios were less than 1.0.

Workers at IBM (1971) have produced some distance-amplitude data for PKP, but from only one station, LASA.

Qamar (1973) has investigated the structure of PKP phases near 140° and has reported amplitudes for five events. These are not enough to give a good average distance-amplitude curve, but the careful readings by Qamar and others of the many near-simultaneously arriving phases has enabled us to better interpret the ISC data we have used to determine our distance-amplitude curve. This curve may be used to determine magnitudes. It may also be used to scale codas in order to determine the opportunities for hiding explosions in world-wide earthquakes.

Figure 1a is a portion of the Jeffreys-Bullen travel-time distance curves, using their nomenclature and showing that the first arrival, P, changes to diffracted P at approximately 105°. The amplitude is

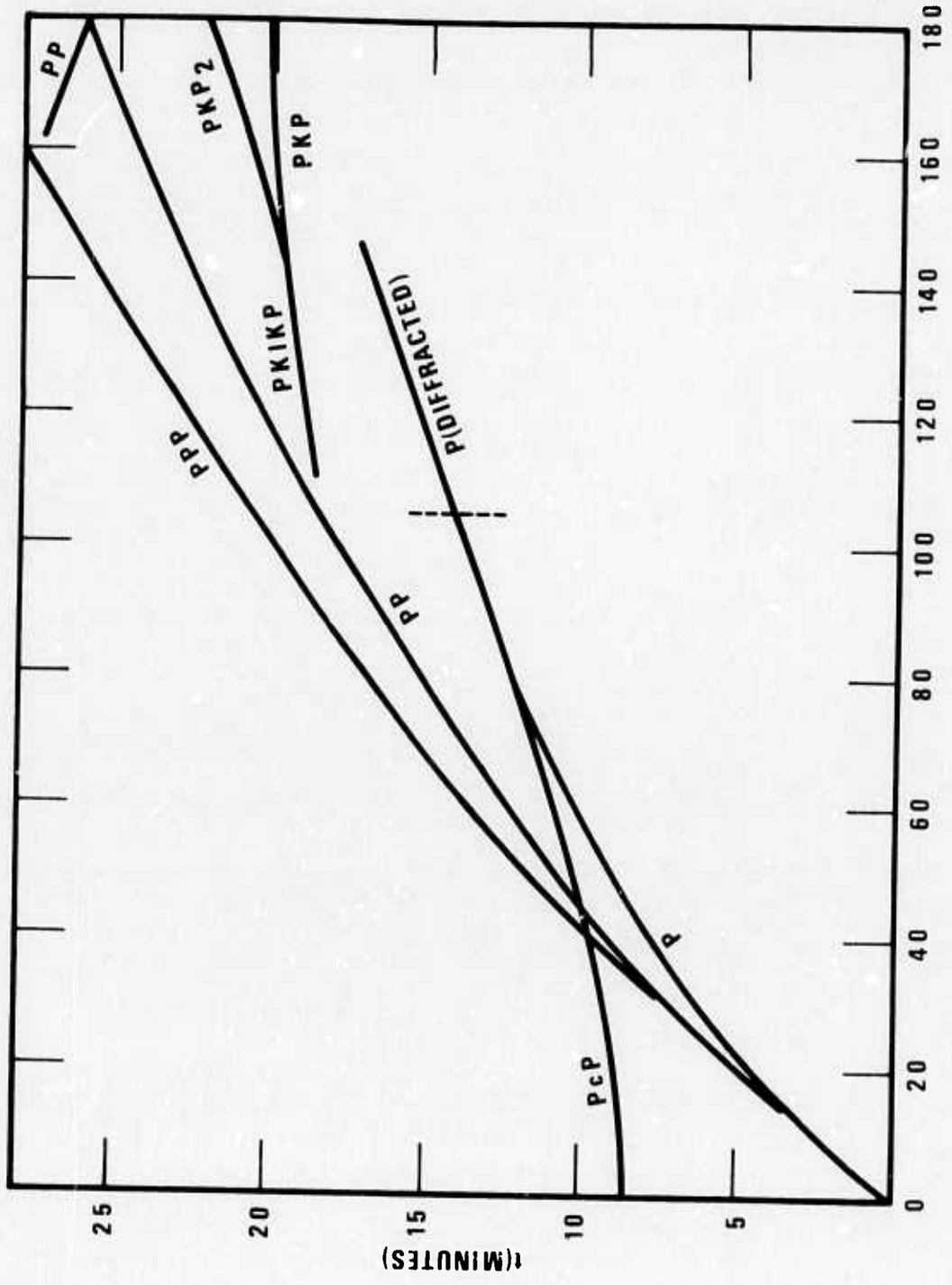

Figure 1a. Travel-time figures for compressional phases.

then greatly reduced, the period lengthens to approximately two seconds, and between 105° and 110° we have the classical shadow zone. In this zone, the largest amplitude wave is PP, a compressional wave singly reflected at the surface. On short period instruments its period is characteristically greater than two seconds, and thus it can not obscure the P signal of another earthquake as easily as might be expected from its amplitude.

At 110° the phase PKIKP (sometimes called PKP, P', P'', or P'_{DF}) begins and the situation rapidly becomes complicated and controversial. Figures 1b and 1c form the basis for the following clear description of the basic core phases by Adams and Randall (1964):

"The ray which leaves the focus at the shallowest angle necessary to enter the core corresponds to A, and successively steeper rays trace the travel-time curve ABCDEF, and have paths through the Earth as shown in Figure 1b, in which the points of emergence of rays that correspond to the points labelled in Figure 1c are shown by dashed letters. Rays corresponding to the branches AB and BC penetrate only the outer core, the branch CD represents rays which undergo total internal reflection at the boundary of the inner core, and rays that represent the branch DF penetrate the inner core; the point F thus corresponds to a ray travelling diametrically through the Earth. The cusp at B is a caustic, and is therefore associated with large amplitudes."

Figures 2a from Ergin (1967) and Figure 2b (drawn from data in Qamar, 1973) give a more detailed picture and some indication of the existing uncertainty and confusion in nomenclature. Our detailed discus-

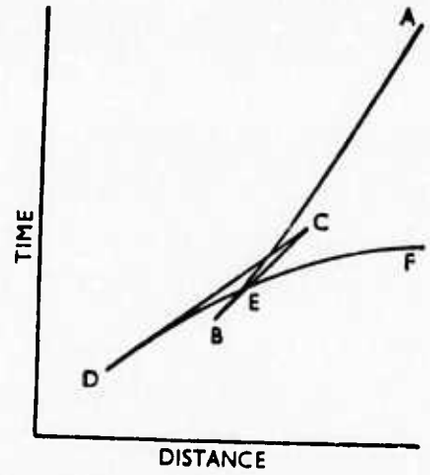

Figure 1b. Travel-time figures for compressional phases.

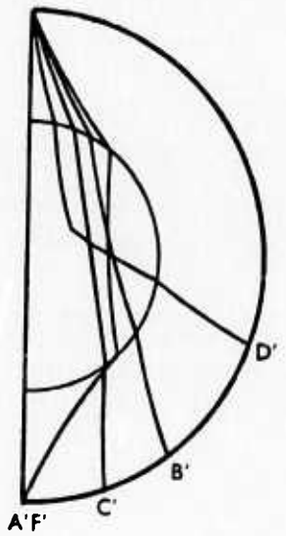

Figure 1c. Travel-time figures for compressional phases.

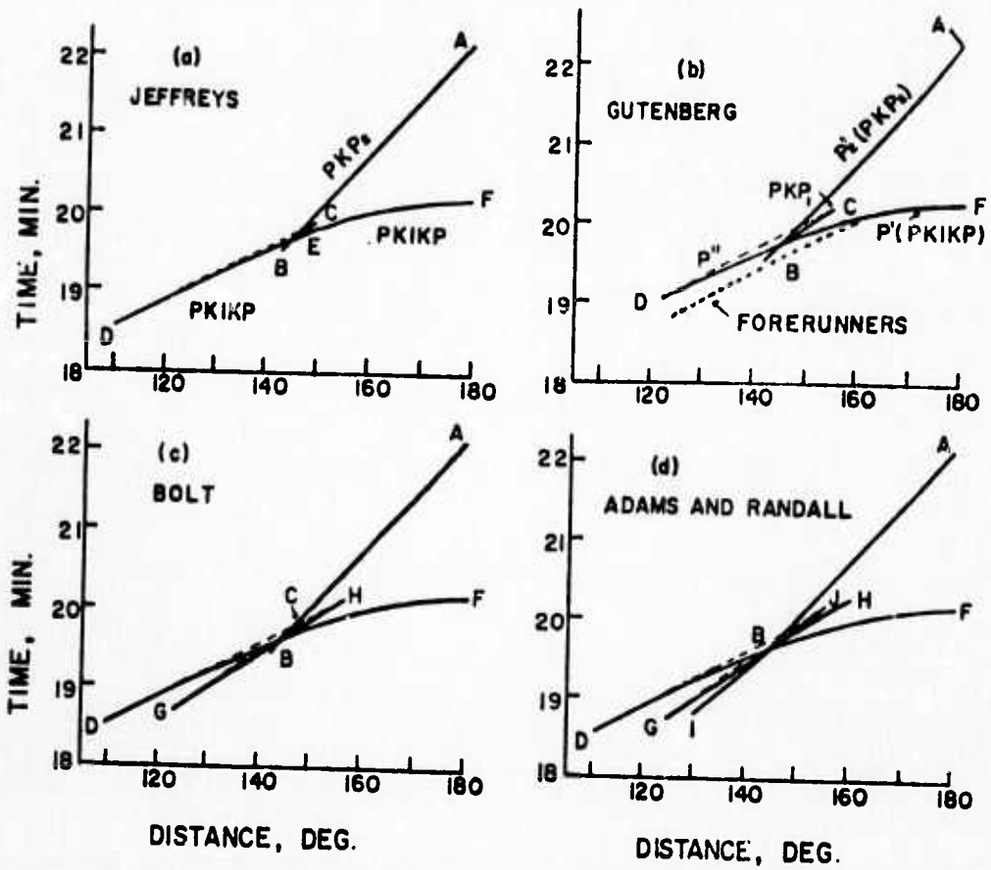

Figure 2a. Travel-time curves for different core models. From Ergin (1967).

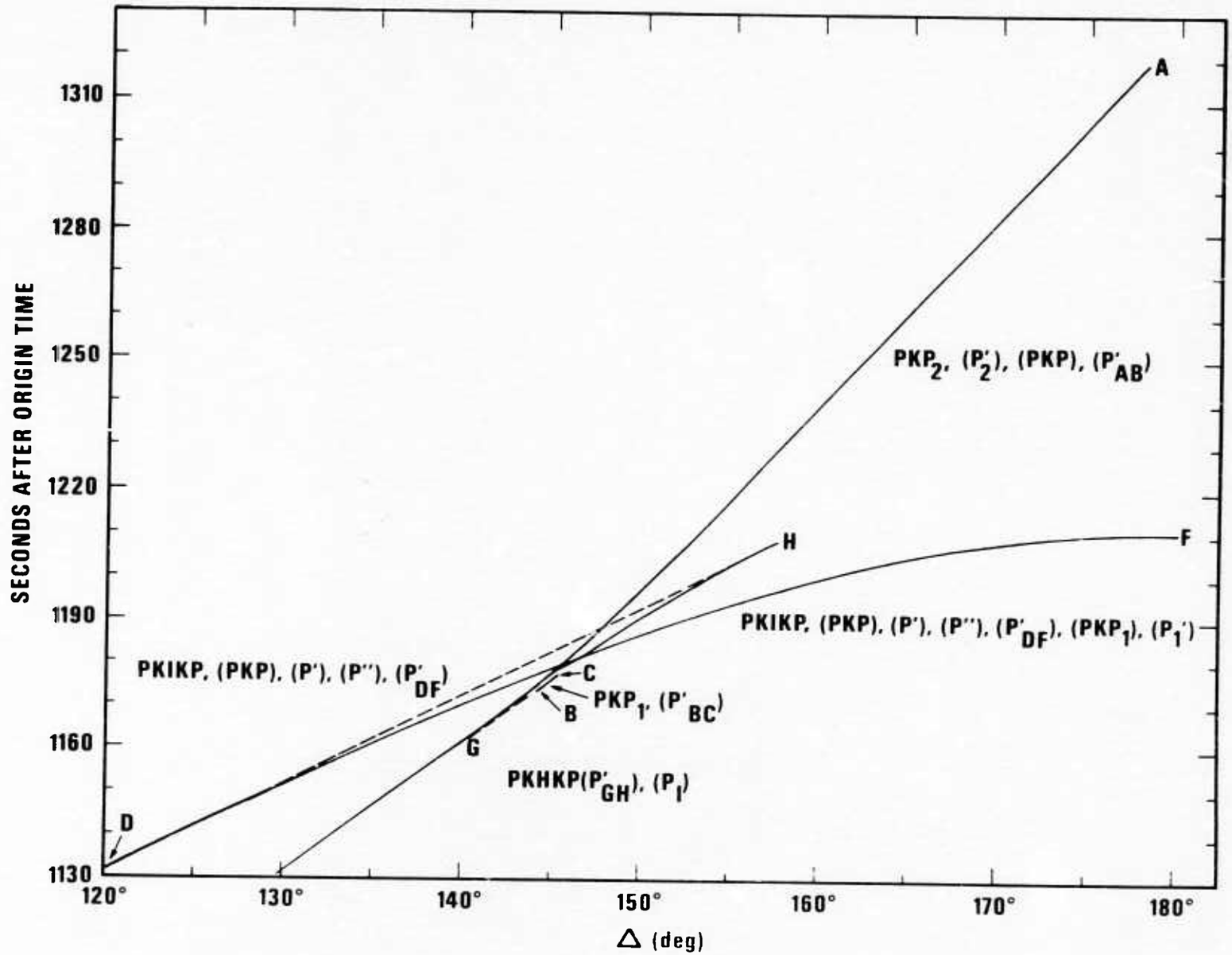

Figure 2b. Qamar's (1973) PKP travel-time-velocity model KOR5. Branch names are ordered approximately by frequency of use. Note conflict for PKP_1.

sions of this distance range will generally be in terms of Qamar's travel time data. While PKIKP is a wave which has traveled through the inner core and is fairly strong, PKiKP (a reflection from the inner core) replaces it at smaller distances and is very weak. PKHKP (also called P_I or P'_{GH}) begins around 125° and is, at first, very weak; so that for the range 110°-140° one may generally be confident that PKIKP is the first arrival phase being read by the average observer at the average site, although for a large event P_{diff} and PKHKP will be observed. PKP_2 (also called P'_2) begins at 143°-144° and both it and PKHKP arrive within a few seconds of PKIKP. So from 140° to 150° it is difficult to know what phase the average observer has measured if he picks the maximum amplitude in the first few seconds of the signal. At distances greater than 150° it is generally possible to decide if the measured phase is PKP_2 by the reported arrival time, although PKIKP may still be confused with PKHKP out to perhaps 157°, where the latter's amplitude sharply decreases.

DATA SELECTION

Our principal data base consists of the International Seismological Centre (ISC) bulletins January-June 1970. Every shallow ($h<70$ km) event was used for which there were two or more $\log_{10}(A/T)$ values reported for $\Delta>110°$. In this time period the ISC reported $\log_{10}(A/T)$ values only for the first arrivals; and by their definitions these would be P to 105°, P_{diff} between 105° and 110°, and PKIKP to 180°. On occasion we would decide on the basis of time residuals whether a phase was PKIKP or if the first motion had been missed and the analyst had actually picked PKP_2 as first motion. In this way it was possible to obtain PKP_2 amplitude data from the ISC bulletin when PKIKP would be the true first motion.

Average B factors were computed by subtracting the $\log_{10}(A/T)$ value from the ISC m_b value, averaging the resulting values over 2.5° increments of distance, and then plotting this average at the mid-point of the 2.5° increments. The same averaging procedure was used for the Geotech data sources used in this report.

In the region between perhaps 100°-120°, PP has a larger short-period amplitude than the first arrival. To obtain these PP amplitudes it was necessary to use other data sources than the ISC since, as mentioned above, they report $\log_{10}(A/T)$ only for the first arrivals. We chose to use the data of Geotech (1963-1968) consisting of phase readings at BMO, CPO, TFO, UBO and WMO between July 18, 1963 and December

31, 1968. Another Geotech data source consisted of the station bulletins of the Long-Range Seismic Measurements Program (1962-1967). For those events from August 18, 1963 through December 1967 which had two or more phase readings for distances greater than 110° we reviewed the NOAA Earthquake Data Reports to find if the reported m_b values were reliable. We required that there be three or more amplitudes reported and used in the magnitude determination in the distance interval $20° < \Delta < 105°$. If amplitudes for $\Delta < 20°$ had been used in the magnitude determination, we removed them and recomputed the magnitudes. Also we generally used, in the recomputed magnitudes, the reported amplitude values which the NOAA had discarded as outlying values. Discarding the amplitudes for $\Delta < 20°$ is generally a wise procedure since Gutenberg's B factors, used by NOAA, are not accurate for these distances; see for example Veith and Clawson (1972). Using outlying magnitudes is justified because, if looked at in terms of a log-normal distribution, one can not usually reject the hypothesis that the outliers are members of the overall population. In any event only 9 event magnitudes were changed and by an average amount of -.25 m_b. These, then, were the magnitudes from which the $\log_{10}(A/T)$ values were subtracted to determine the PP distance-amplitude relation.

Appendix I presents the 135 earthquakes used with the ISC data and Appendix II is the same for the 45 earthquakes used with the Geotech data used to determine the PP amplitudes.

RESULTS

Figure 3 gives the principal results of the present work as curves drawn by hand through the ISC data of amplitude versus distance for P, P_{diff}, and several compressional core phases. Table I and II give the corresponding "B" factors. A straight line approximation to the Geotech PP data is also shown.

Between 90° and 100° the curve is in good agreement with Veith and Clawson's (1972) distance-amplitude curve for a depth of 40 km (corrected for reference to zero-to-peak amplitudes) suggesting that the ISC data used have no substantial bias. In the distance interval $90° < \Delta < 105°$ the only ISC data used was 01 April through 08 April 1970, and the full months of May and June since more than enough data was available during the smaller time period for our purposes.

In the upper portion of Figure 3 we give the number of observations for each phase in each 2.5° interval. The averages over these intervals are given as points in Figures 3 and 4. The smooth curve in Figure 4 is the same as in Figure 3. It is apparent that the erratic average values are for intervals where there are few data points. We note that the first motion does not recover to its amplitude at 90°-95° until about 143°.

In Figure 4 we see that the scatter in amplitudes is quite large. A typical standard deviation, assuming a log-normal distribution, is about 0.35

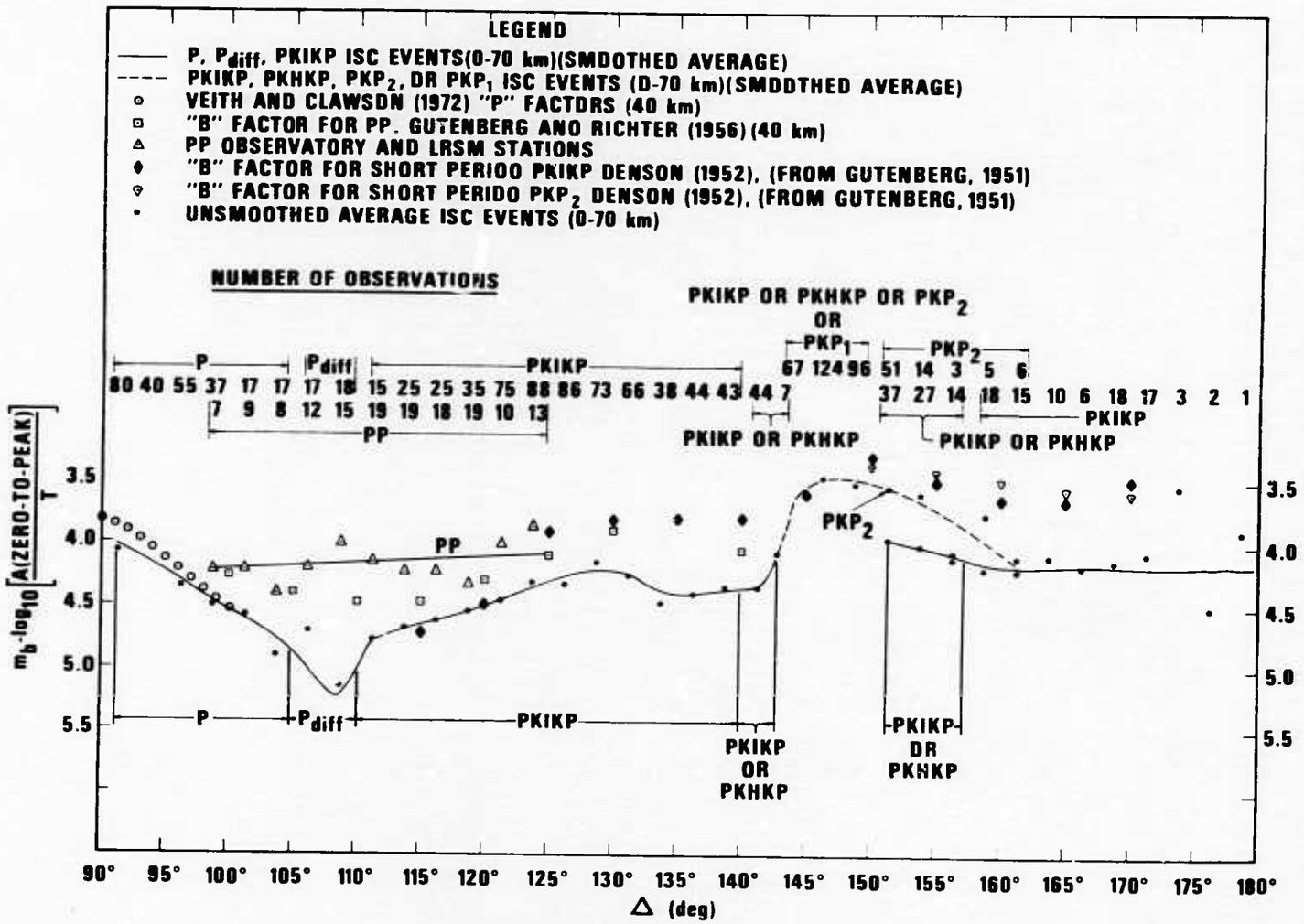

Figure 3. Average amplitude versus distance curves from ISC event data (90°-180°).

TABLE I

Table of Distance Factors (B) for Shallow Events for Phases P, P_{diff}, PKIKP or PKHKP, and PKP_2 (from Figures 3 and 4)

Phase	Distance (deg)	B
P	92	4.065
	93	4.120
	94	4.175
	95	4.230
	96	4.300
	97	4.360
	98	4.425
	99	4.480
	100	4.535
	101	4.590
	102	4.640
	103	4.705
	104	4.780
	105	4.860
P_{diff}	106	4.980
	107	5.125
	108	5.225
	109	5.200
	110	5.025
PKIKP	111	4.820
	112	4.750
	113	4.715
	114	4.675
	115	4.650
	116	4.630
	117	4.600
	118	4.570
	119	4.530
	120	4.490
	121	4.460
	122	4.425
	123	4.385
	124	4.350
	125	4.315
PKIKP	126	4.280
	127	4.250
	128	4.225
	129	4.215
	130	4.225
	131	4.250
	132	4.290
	133	4.350
	134	4.390
	135	4.410
	136	4.410
	137	4.400
	138	4.390
	139	4.375
	140	4.365
PKIKP or PKHKP	141	4.350
	142	4.250
	143	4.015
PKIKP or PKHKP	144	3.650
	145	3.510
	146	3.490
	147	3.475
PKP_2 or PKP_1	148	3.480
	149	3.500
	150	3.525
	151	3.550
PKIKP or PKHKP	152	3.980
	153	4.010
	154	4.035
	155	4.060
	156	4.075
	157	4.100
PKIKP	158	4.140
	159	4.170
PKIKP	160	4.175
	161	4.185
	162	4.185
	163	4.185
	164	4.175
	165	4.175
	166	4.175
	167	4.175
	168	4.170
	169	4.160
	170	4.160
	171	4.160
	172	*
	173	*
	174	*
	175	*
	176	*
	177	*
	178	*
PKP_2	152	3.575
	153	3.630
	154	3.685
	155	3.725
	156	*3.800
	157	*3.860
	158	3.925
	159	4.000
	160	4.065
	161	4.150

$$\log_{10}\left(\frac{A(\text{zero to peak})}{T}\right) = M_b - B$$

* 3 observations or less

TABLE II

Table of Distance Factors (B) for Shallow Events for the Phase PP (from PP Average Figure 3)

Δ(deg)	B	Δ(deg)	B
99	4.220	113	4.150
100	4.215	114	4.145
101	4.210	115	4.140
102	4.205	116	4.130
103	4.200	117	4.125
104	4.195	118	4.120
105	4.190	119	4.115
106	4.185	120	4.115
107	4.180	121	4.110
108	4.175	122	4.105
109	4.170	123	4.100
110	4.165	124	4.090
111	4.160	125	4.085
112	4.155		

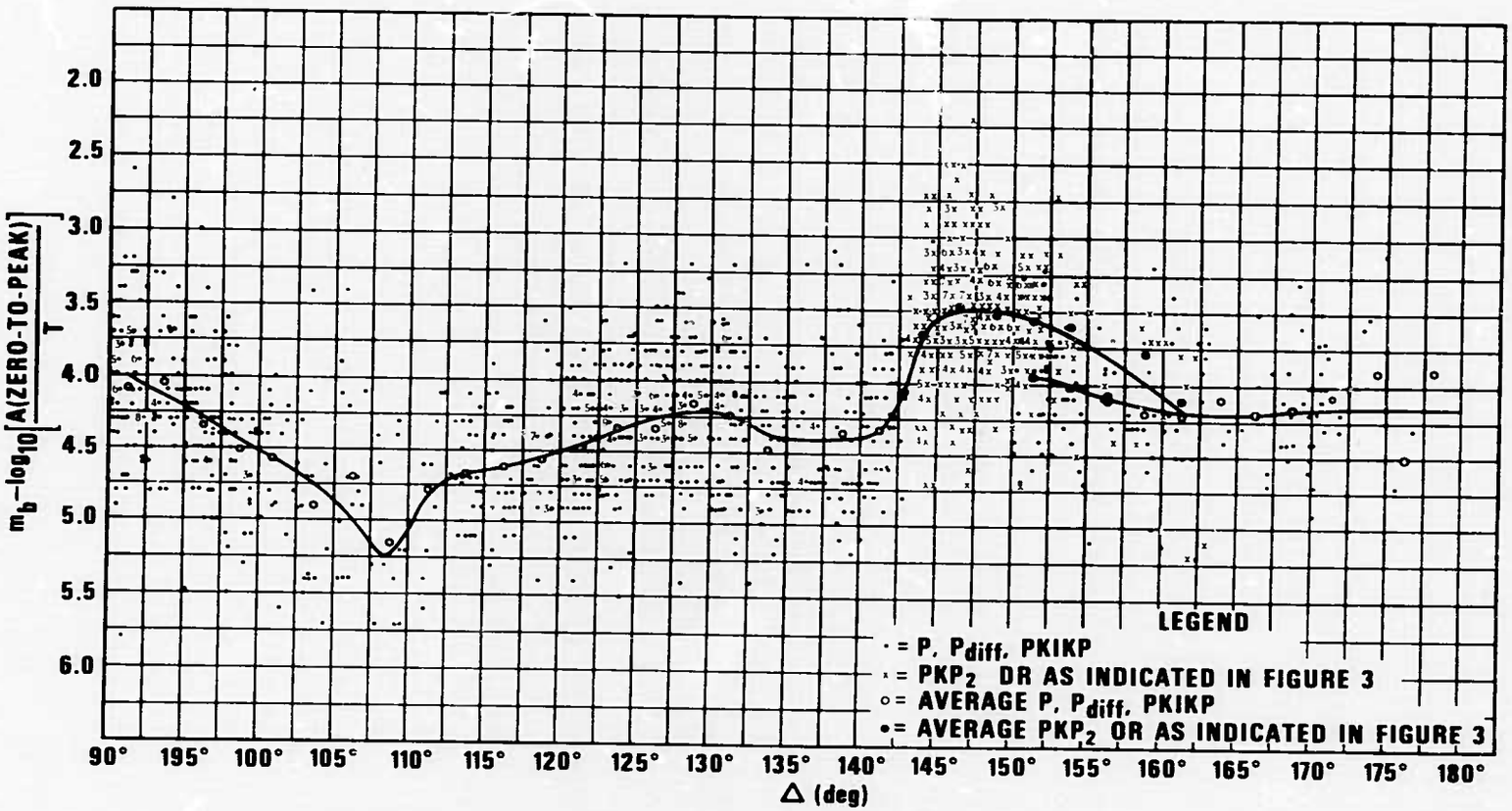

Figure 4. Individual amplitude versus distance values from ISC reports (90°-180°), 01 January - 30 June 1970.

magnitude units. We must remember, however, that this variance includes the variance of the event P wave m_b values with respect to the average "PKP" m_b. (Of course each event's P wave m_b value may also have a small standard deviation of the mean.) This variance may be non-zero because for any particular event the "PKP" m_b, sampling as it does a different portion of the focal sphere, may have a mean substantially different from the P wave m_b. However, over an ensemble of earthquakes with different focal mechanisms, a suitably defined PKP m_b should approach the P wave m_b.

We might speculate that had our m_b values been determined from PKP readings, the observed variance would have been less than 0.35. However, we may note that when Veith and Clawson (1972) computed the standard deviation of their P-wave data (normalized by P-wave magnitudes from their own P-wave distance-amplitude curve) they obtained $\sigma = 0.356$ over the distance interval 25°-90°. This is not significantly different from the value of 0.35 we find between 90° and 180°. This indicates either that PKP has a smaller variance about its mean amplitude than does P, or that the network PKP m_b can be expected to be very close to the network P-wave m_b for individual events.

On Figure 3 we have plotted "short-period" PKIKP and PKP_2 points from Denson (1952). The disagreement

is substantial; but since his entire curve comes from a total of only 92 points, since his instrumentation was so different, and since his station set was restricted to Pasadena, one station in Mexico, and two in South America, we believe our curves are more reliable as a world-wide average. Something of Denson's instrumentation problems are suggested by the fact that for $\Delta>130°$ he found $1.5 \lesssim T \lesssim 2.5$ seconds whereas our ISC data are invariably in the period range $0.8 \lesssim T \lesssim 1.5$ seconds. Figure 5 from Subiza and Båth (1964) reinforces this point by showing that the PKIKP mean period is 0.88 seconds for $120°<\Delta<150°$.

Also in Figure 3 we see that for our straight line interpretation of the PP data in the interval 100°-125°, PP is between 0.2 and 0.9 magnitude units larger in A/T than the first motion; P, P_{diff}, or PKP. Since for PP, T is typically two seconds, A itself is perhaps 0.3 magnitude units even larger. For weak events it should, therefore, be a useful phase for magnitude determination. The PP curve was determined with the Geotech amplitude data, as mentioned in the prior section on data, but there are some problems in its use. Evernden and Clark (1970) have pointed out that the quiet stations in the United States generally record smaller P-wave amplitudes than the noisy ones. Since the Observatory and LRSM stations, from which the Geotech data are gathered, were preferentially located in quiet sites, their PP amplitudes are also likely to be too small on the average.

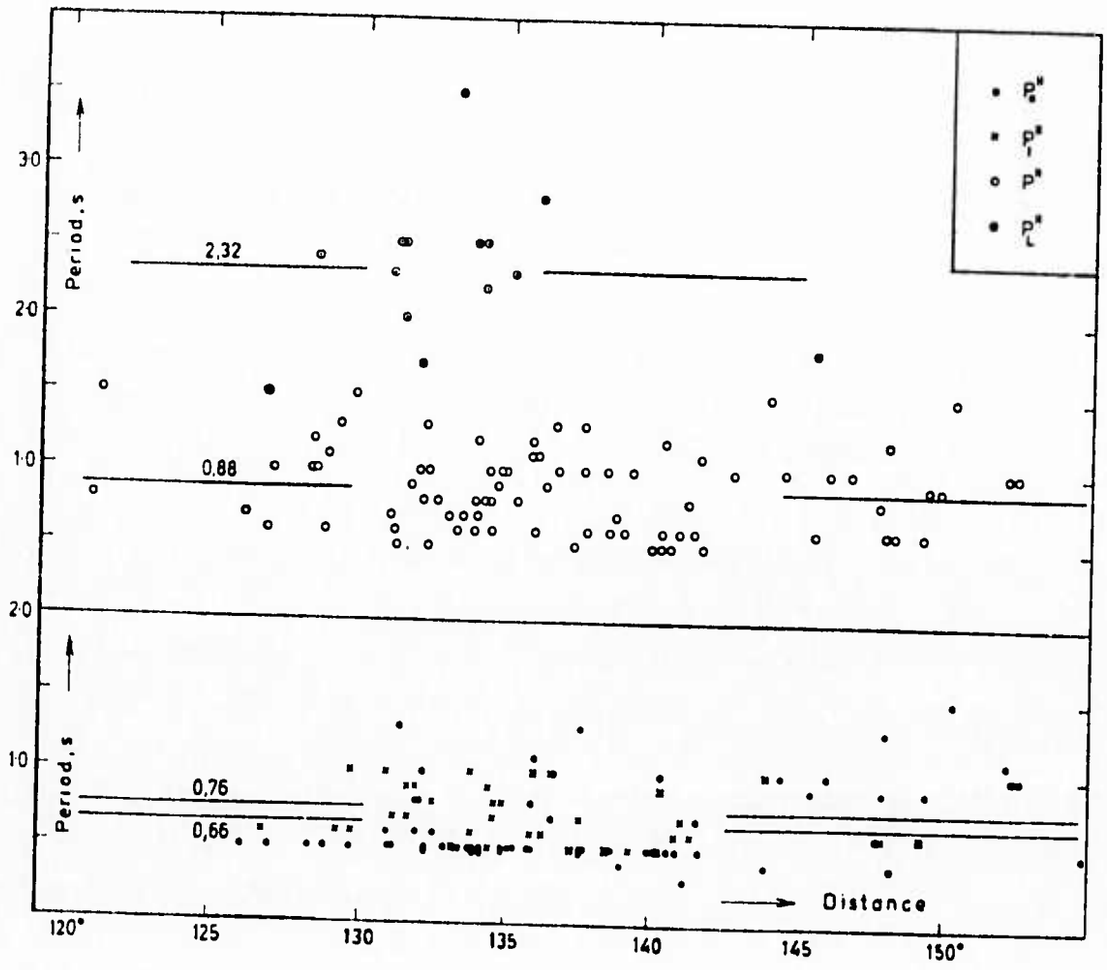

Figure 5. Period as a function of distance for PKIKP (P'') from Subiza and Bath (1964).

As an illustration, Figure 6 shows that as a function of distance there is a difference of 0.1 - 0.8 magnitude units between the average first arrival amplitudes reported by the Observatories and by NOAA reporting stations found in the Earthquake Data Reports.

Thus, when most of one's data set comes from unusually quiet stations it is necessary to allow for station effects.

In Figure 7 we have plotted the average P, P_{diff}, PKP curve; and the PP curve from the Appendix II events for LRSM and Observatory data. To transfer the data to Figure 3 we assume that station-network effects account for the difference between the P, P_{diff}, PKP curves in Figures 3 and 7; and therefore place the PP curve of Figure 7 above the P, P_{diff}, PKP curve in Figure 3 by an amount equal to its distance above the Figure 7 P, P_{diff}, PKP curve. Also in Figure 3 we have plotted a few points from Gutenberg and Richter (1956) for PP. While we find A/T values as much as 0.35 units larger than did Gutenberg and Richter, the overall agreement is probably fairly good considering the differing instrumentation.

Figure 8 presents the scatter in the PP amplitudes. The standard deviation is about 0.45 magnitude units, significantly larger than for P, PKP, et al. This can probably be traced to the vagaries of the free reflection surface; or to the fact the PP is

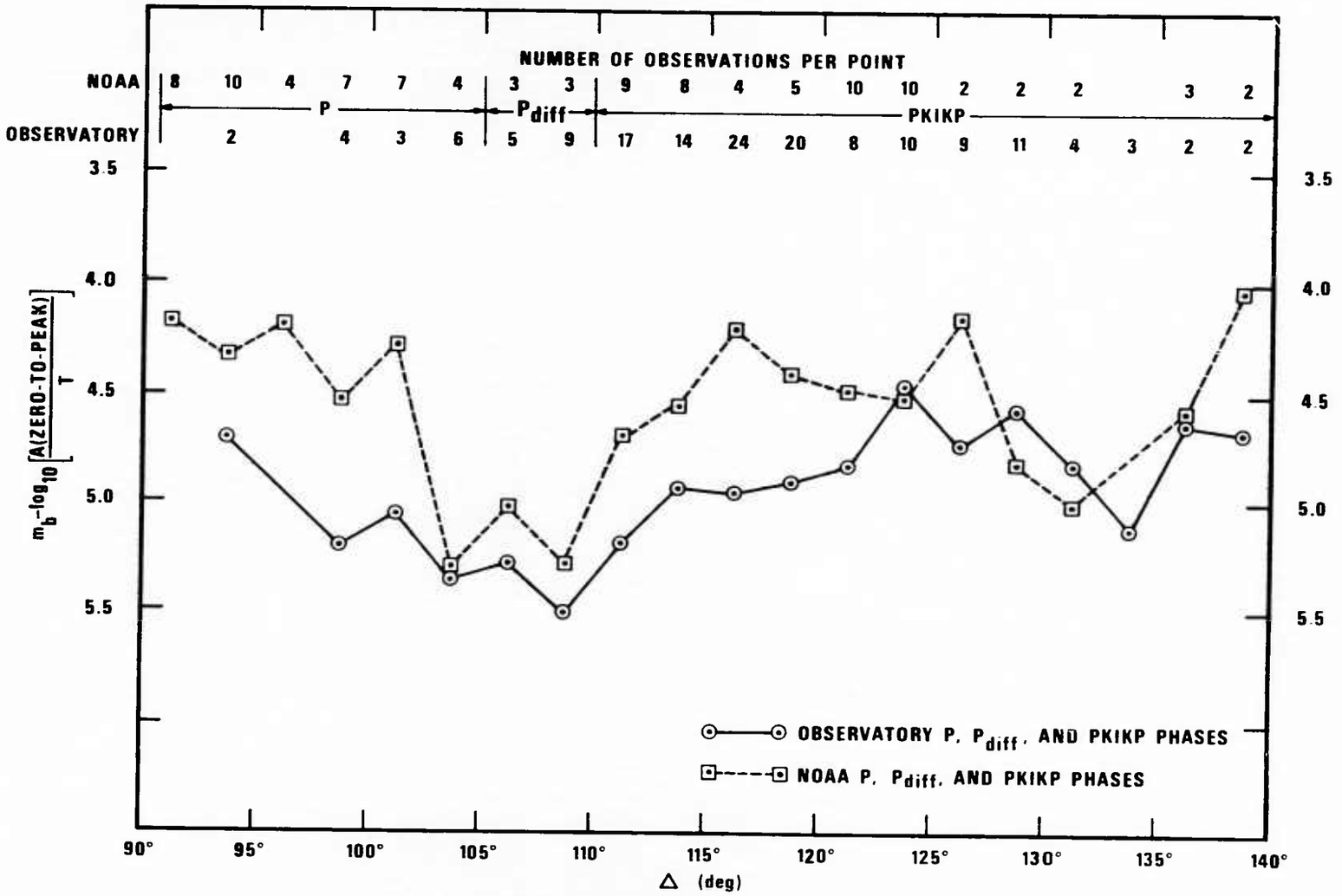

Figure 6. Average amplitude versus distance curves (90°-140°) for P, P_{diff}, and PKIKP; showing the bias between the quieter Observatory Stations and the other NOAA reporting stations.

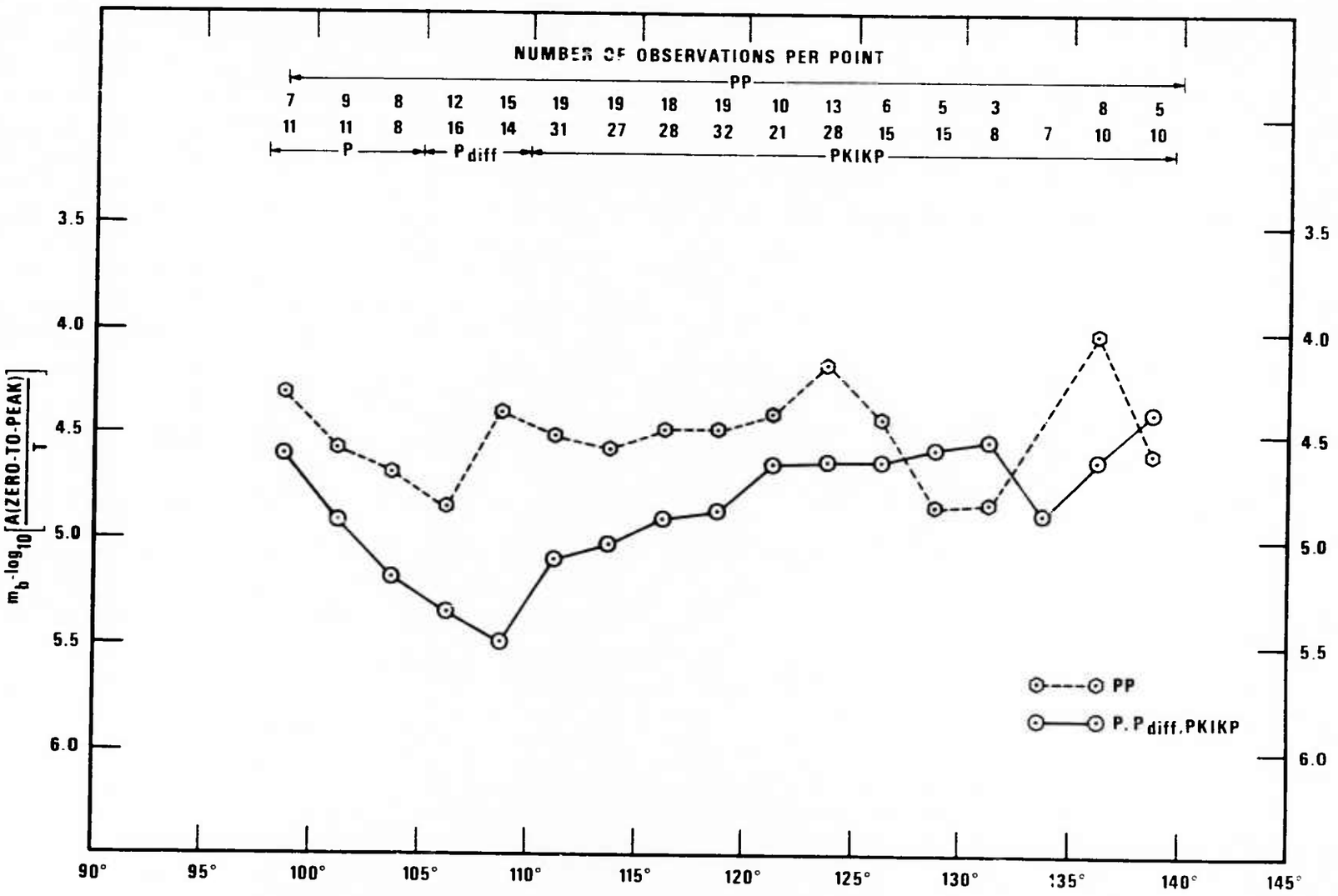

Figure 7. Average amplitude versus distance curves from Observatory and LRSM event data for P, P_{diff}; PKIKP, and PP (90°-138°).

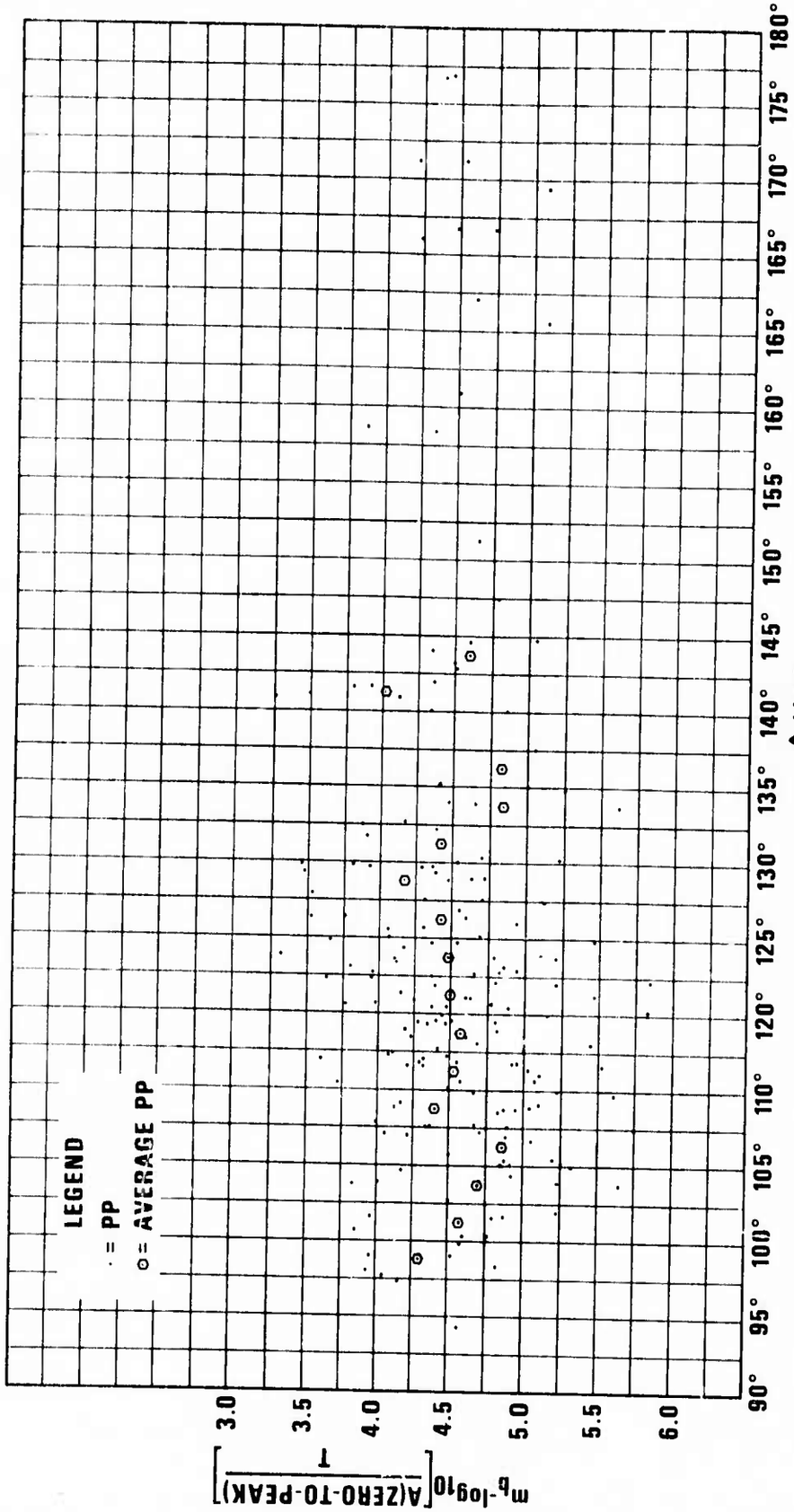

Figure 8. Individual amplitude versus distance values for PP from Observatory and LRSM readings (90°-180°) 18 July 1963 - 31 October 1968.

an emergent phase and that analysts are not so practiced in detecting it, which may lead to erroneous or inconsistant measurements. A final possibility is that the NOAA magnitudes for these events are not as reliable as the ISC magnitudes for the events in Appendix I.

Figure 9 gives Qamar's (1973) careful phase-amplitude measurements for a single event. We see that in the range 142°-155° the dominant amplitudes are from the GH branch (see Figre 2b) i.e. PKHKP, (P'_{GH} or P_I).

Figure 10 compares the average curves from Figure 3 with IBM data (1971). We see that the agreement is satisfactory considering the fact that the IBM data is all from a single station and therefore will have biases due to station effects and due to the fact that in any specific distance interval a large proportion of the events are from only a few epicentral regions. In addition, the IBM data includes deep events, whereas we restricted ourselves to those shallower than 70 km.

Figure 11 is Shurbet's (1967) plot of his data, normalized to 1.0 at 125°. We see that the agreement with our curve, also normalized at 125° is excellent except that our amplitudes are perhaps 0.2 magnitude units high between 148° and 158°. Shurbet attempted to distinguish PKIKP, PKHKP and PKP_2 in this distance interval. Thus this discrepancy could be explained

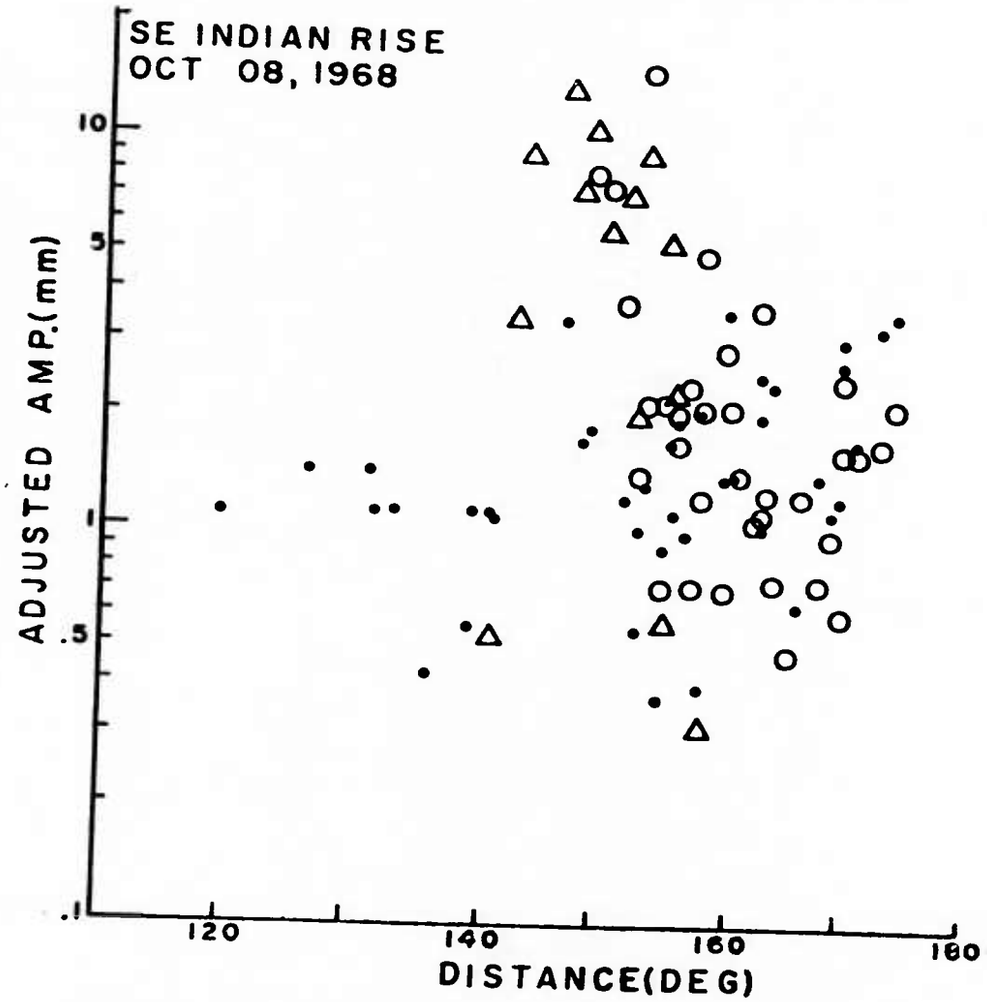

Figure 9. WWSSN station amplitudes reduced to a magnification of 25,000 at 1 cps. Amplitudes are not adjusted for period. Small dots are P_1, open circles P_2, triangles P_I (or GH branch). From Qamar, 1973.

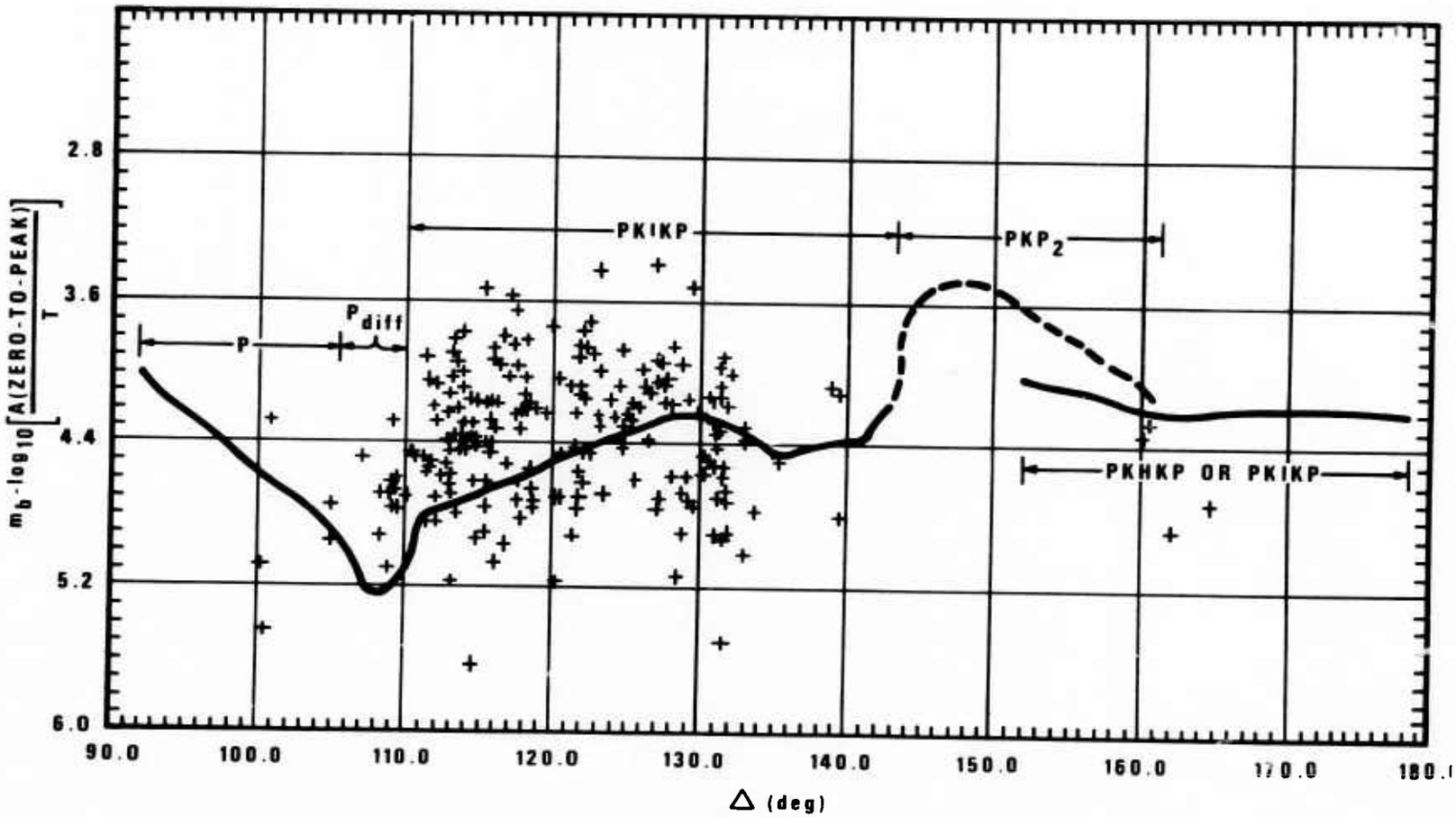

Figure 10. Average amplitude versus distance curves from ISC event data (90°-180°) 01 January - 30 June 1970 compared to the single station (LASA) individual values from IBM (1971).

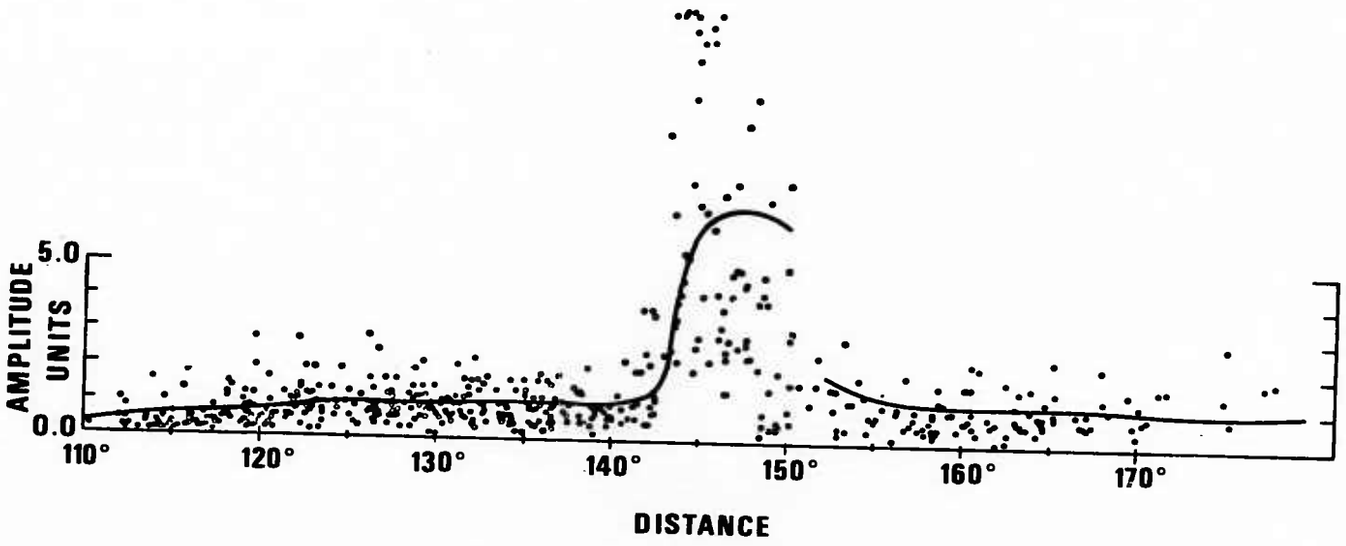

Figure 11. Average amplitude versus distance curves from ISC event data (110°-180°) 01 January - 30 June 1970 compared to normalized PKIKP data from Shurbet (1967).

if in the distance range $148° < \Delta < 158°$ he sometimes successfully rejected PKHKP and PKP_2, while for $150° < \Delta < 158°$ he sometimes successfully rejected PKHKP.

CONCLUSIONS AND SUGGESTIONS FOR FURTHER RESEARCH

The distance-amplitude curves obtained in this report for $\Delta>90°$ are thought to be more accurate and complete than any heretofore published. They should be of substantial use for determining more accurate m_b values and for determining the number of opportunities for masking explosions in earthquakes more distant than 90° from a candidate detecting station. A substantial reduction in the scatter of the data about these curves, e.g. in the P_{diff} region and for $\Delta>170°$, could be obtained by using more of the available ISC data. This might be efficiently accomplished using the sorting and selection procedures we have developed in this paper to write a computer program which would operate on magnetic tape data available from the ISC. Using only the larger events from the complete data set will enable us to evaluate the effect on the distance-amplitude relations caused by the fact that, for weak events, the stations at which a phase arrives with unusual strength are more apt to report. It will also be useful to compute station corrections and use them to reduce the scatter in the data, although the work of von Seggern (1973) suggests that there will be little net effect.

REFERENCES

Adams, R. D., and Randall, M. J., 1964, The fine structure of the Earth's core: Bull. Seism. Soc. Am., v. 54, p. 1299-1313.

Cohen, T. J., Sweetser, E. I., and Dutterer, T. J., 1972, P and PKP coda decay characteristics for earthquakes: Seismic Data Laboratory Report No. 301, Teledyne Geotech, Alexandria, Virginia.

Denson, M. E., Jr., 1952, Longitudinal waves through the earth's core: Bull. Seism. Soc. Am., v. 42, no. 2, p. 119-134.

Engdahl, E. R., 1968, Core phases and the Earth's core, Ph.D. Thesis, Department of Geophysics, St. Louis University, St. Louis, Missouri.

Ergin, K., 1967, Seismic evidence for a new layered structure of the Earth's core: J. Geophys. Res., v. 72, p. 3669-3688.

Evernden, J. F., and Clark, D. M., 1970, Study of teleseismic P: Physics of the Earth and Planetary Interiors, v. 4, no. 1, p. 1-31.

Geotech, 1962-1967, Seismological bulletin long-range seismic measurements program: Teledyne Geotech, Garland, Texas.

Geotech, 1963-1968, The registration of earthquakes at Blue Mountains Seismological Observatory, Cumberland Plateau Seismological Observatory, Tonto

Forest Seismological Observatory, Uinta Basin Seismological Observatory, and Wichita Mountains Seismological Observatory: Teledyne Geotech, Garland, Texas.

Gutenberg, B., 1951, PKKP, P'P' and the earth's core: Trans. Am. Geoph. Un., v. 32, p. 373-390.

Gutenberg, B., and Richter, C. F., 1956, Magnitude and energy of earthquakes: Annali de Geoficica, v. 9, p. 1-15.

IBM, 1971, Integrated seismic research signal processing system: Tenth quarterly technical report, Contract F19628-68-C-0400, ESD-TR-72-123, p. 68-119.

Qamar, A., 1973, Revised velocities in the earth's core: Bull. Seism. Soc. Am., v. 63, no. 3, p. 1073-1106.

Richter, C. F., 1958, Elementary seismology, Freeman, W. H., San Francisco.

Ruprechtova, L., 1972, Recent interpretation of the core discontinuities: Zeitschrift für Geophysik, v. 38, p. 441-446.

Shahidi, M., 1968, Variation of amplitude of PKP across the caustic: Phys. Earth Planet. Interiors, v. 1, p. 97-102.

REFERENCES (Continued)

Shurbet, D. H., 1967, The earthquake P phases which penetrate the earth's core: Bull. Seism. Soc. Am., v. 57, p. 875-890.

Subiza, G. P., and Båth, M., 1964, Core phases and the inner core boundary: Geophy. J., v. 8, p. 496-513.

Sweetser, E. I., and Cohen, T. J., 1973, Average P and PKP coda characteristics for earthquakes: Seismic Data Laboratory Report No. 305, Teledyne Geotech, Alexandria, Virginia.

Veith, K. F., and Clawson, G. E., 1972, Magnitude from short-period P-wave data: Bull. Seism. Soc. Am., v. 62, no. 2, p. 435-452.

APPENDIX I

ISC Events (0-70 km)
01 Jan 70 thru 30 Jun 70

ISC Events (0-70 km)

01 Jan 70 Thru 30 Jun 70

Date	Origin Time	Latitude	Longitude	Depth (km)	ISC m_b	Geographical Region	Number of Phase Readings obtained from each event P	PD	PKP	PKP_1	PKP_2
01 Jan 70	17:11:00.3	29.6S	177.3W	43	5.3	Kermadec Islands			7	5	4
05 Jan 70	00:20:13.7	19.2N	121.2E	41	5.4	Philippines			2	2	1
06 Jan 70	05:35:52.0	9.6S	151.5E	8	5.7	East of New Guinea		1	16		5
09 Jan 70	04:42:58.0	33.6S	179.2W	31	5.1	South of Kermadec Islands			6	2	3
09 Jan 70	23:16:20.6	9.3S	117.3E	58	5.7	Sumbawa Island			6	3	1
10 Jan 70	12:07:08.6	6.8N	126.8E	68	5.9	Mindanao, Philippines			2	3	2
11 Jan 70	03:14:24.0	6.2S	71.3E	33	4.9	Chagos Archipelago			2	1	2
11 Jan 70	05:19:38.1	22.6S	171.4E	50	5.2	Loyalty Islands			6		9
18 Jan 70	00:18:24.4	21.4N	146.7E	42	5.7	Mariana Islands			10		1
18 Jan 70	04:10:46.0	15.6S	179.9W	45	5.1	Fiji Islands			3		3
20 Jan 70	00:38:25.0	53.8N	163.6W	33	5.1	Unimak, Aleutian Islands			2		4
21 Jan 70	17:51:37.4	7.0N	104.2W	23	6.1	Off Coast of Central America	1		8	2	2
23 Jan 70	03:31:29.3	53.7N	163.6W	36	5.2	Unimak, Aleutian Islands			2		4
24 Jan 70	21:55:39.3	19.1S	168.8E	68	4.7	New Hebrides			4		4
26 Jan 70	10:01:20.0	12.6S	166.4E	42	5.6	Santa Cruz Islands			9		
27 Jan 70	09:02:52.9	10.9S	165.9E	59	5.5	Santa Cruz Islands			9		
04 Feb 70	05:08:48.0	15.6N	99.5W	18	5.9	Coast of Guerrero, Mexico			8		1
04 Feb 70	22:45:58.3	22.7S	171.4E	54	5.2	Loyalty Islands			4	3	2
05 Feb 70	12:46:39.2	47.0N	154.1E	39	5.4	Kurile Islands			6		1
05 Feb 70	22:05:58.5	12.6N	122.1E	8	5.9	Luzon, Philippines	1		3	5	3
06 Feb 70	00:11:40.5	54.6N	163.6E	43	5.6	Coast of Kamchatka			7		
06 Feb 70	02:17:33.5	12.7N	121.9E	34	5.3	Mindoro, Philippines			2		4
07 Feb 70	10:01:06.0	47.3N	154.0E	32	5.3	Kurile Islands			6		1

Date	Origin Time	Latitude	Longitude	Depth (km)	ISC m_b	Geographical Region	Number of Phase Readings obtained from each event				
							P	PD	PKP	PKP_1	PKP_2
11 Feb 70	01:59:53.6	21.0S	174.0W	33	5.1	Tonga Islands			5	1	5
14 Feb 70	11:17:16.4	9.8S	75.6W	36	5.8	Peru			2	2	1
17 Feb 70	04:10:20.4	56.0S	27.3W	33	5.1	South Sandwich Islands			4	2	3
17 Feb 70	19:14:22.6	22.4S	170.4E	46	5.4	Loyalty Islands			2	1	5
17 Feb 70	01:44:18.0	36.2S	53.1E	33	5.2	South Indian Ocean			2	5	5
19 Feb 70	10:47:38.3	30.4S	177.8W	43	5.4	Kermadec Islands			9	3	6
24 Feb 70	15:08:37.4	7.1S	155.6E	60	5.3	Solomon Islands			15		1
26 Feb 70	23:25:00.0	16.5S	173.6E	11	5.4	Fiji Islands			5	1	4
28 Feb 70	04:58:11.2	16.1S	172.0W	34	5.3	Samoa Islands				1	7
01 Mar 70	10:04:02.0	28.5S	71.0W	32	5.0	Coast of Central Chile			1		3
02 Mar 70	01:50:55.0	22.5S	174.3W	15	4.8	Tonga Islands			3	1	3
04 Mar 70	03:30:34.0	12.2N	143.8E	21	6.0	South of Mariana Islands			9		6
07 Mar 70	17:11:51.4	22.5S	174.2W	33	5.1	Tonga Islands			4		4
08 Mar 70	11:51:22.3	1.8N	126.7E	56	5.5	Molucca Passage	3	5	2		
09 Mar 70	16:01:11.0	19.1S	168.5E	39	6.0	New Hebrides		15	1	9	
09 Mar 70	18:30:55.0	19.1S	168.4E	27	5.4	New Hebrides		8		9	
10 Mar 70	04:58:26.7	44.7N	149.0E	44	6.2	Kurile Islands		8		1	
10 Mar 70	06:11:56.0	12.6N	122.2E	26	5.6	Luzon, Philippines		4	4	3	
10 Mar 70	17:15:16.6	31.0S	116.7E	63	5.5	Western Australia		4		6	
11 Mar 70	22:38:32.4	57.4N	154.0W	16	6.1	Kodiak, Aleutian Islands		5		3	
13 Mar 70	18:10:30.1	19.1S	168.4E	17	4.8	New Hebrides		2		8	
16 Mar 70	16:25:23.2	19.2S	168.2W	8	4.8	New Hebrides		7		4	
19 Mar 70	23:33:28.7	51.3N	173.8E	8	5.8	Near Islands, Aleutian Islands		4		3	
21 Mar 70	22:32:23.3	21.2S	173.9W	33	5.0	Tonga Islands		5		5	
22 Mar 70	23:01:35.0	53.0S	140.6E	56	4.8	West of Macquarie Island		3	1	8	
24 Mar 70	10:35:16.9	22.1S	126.7E	3	6.1	Western Australia	2	21	4	5	

Date	Origin Time	Latitude	Longitude	Depth (km)	ISC m_b	Geographical Region	Number of Phase Readings obtained from each event				
							P	PD	PKP	PKP_1	PKP_2
27 Mar 70	18:36:47.0	0.3N	119.4E	11	6.0	Northern Celebes			6	3	
28 Mar 70	05:16:15.0	35.2S	54.1E	7	4.9	South Indian Ocean				3	4
28 Mar 70	07:45:59.5	6.3S	154.6E	59	5.8	Solomon Islands			15		2
31 Mar 70	18:18:28.0	3.8S	69.7E	59	5.5	Chagos Archipelago			1		5
01 Apr 70	11:17:43.3	29.2S	61.1E	20	4.7	Atlantic-Indian Ocean Ridge				3	1
02 Apr 70	11:11:42.2	20.4S	173.8W	33	5.6	Tonga Islands	1		5	4	3
03 Apr 70	06:52:34.1	20.5S	174.1W	39	5.5	Tonga Islands	2		1	3	3
03 Apr 70	13:59:02.5	51.9N	175.3W	57	5.0	Andreanof Islands			5		3
03 Apr 70	21:35:52.0	8.3S	126.6E	58	5.2	Timor, Sunda Islands	5		2		2
05 Apr 70	11:10:31.0	17.8S	167.9E	27	4.9	New Hebrides	3		7		7
07 Apr 70	05:34:06.2	15.8N	121.7E	40	6.5	Luzon, Philippines	27	3	2	5	7
07 Apr 70	05:53:48.6	15.5N	122.4E	47	5.6	Luzon, Philippines	7		1	1	
07 Apr 70	06:11:52.8	15.7N	121.9E	22	5.5	Luzon, Philippines	11	1	1	2	2
07 Apr 70	06:34:19.2	15.5N	121.9E	33	5.5	Luzon, Philippines	3	1	1	2	
07 Apr 70	17:59:57.3	15.5N	121.8E	33	5.2	Luzon, Philippines	4			2	
08 Apr 70	14:41:09.2	13.9S	166.8E	70	5.4	New Hebrides	4		12		2
08 Apr 70	21:23:54.0	15.4N	121.8E	7	5.7	Luzon, Philippines		2	1	3	2
09 Apr 70	16:24:30.0	13.3N	92.3W	26	5.3	West Coast of Chiapas, Mexico			3		2
09 Apr 70	21:41:51.8	40.8S	43.3E	28	5.2	Atlantic-Indian Ocean Ridge			1	4	1
11 Apr 70	04:05:42.9	59.7N	142.5W	7	5.3	Gulf of Alaska			6		1
11 Apr 70	06:21:17.0	19.2S	173.5W	33	5.3	Tonga Islands				1	4
12 Apr 70	02:10:36.7	51.5N	178.5W	52	5.2	Andreanof Islands			6		2
12 Apr 70	04:01:44.6	15.1N	122.0E	25	5.8	Luzon, Philippines		2	1	5	3
14 Apr 70	08:27:53.6	5.8S	105.5E	57	5.0	Sunda Strait			3		3
14 Apr 70	13:46:34.0	21.1S	174.4W	64	5.4	Tonga Islands			1	4	2
14 Apr 70	19:08:21.8	33.2S	19.5E	33	5.4	South Africa			2		7

Date	Origin Time	Latitude	Longitude	Depth (km)	ISC m_b	Geographic Region	Number of Phase Readings obtained from each event				
							P	PD	PKP	PKP_1	PKP_2
15 Apr 70	13:14:26.7	15.1N	122.7E	50	5.6	Luzon, Philippines		1	1	3	2
16 Apr 70	05:33:18.2	59.8N	142.4W	7	5.6	Gulf of Alaska			5		1
18 Apr 70	19:22:59.0	53.6N	166.1W	29	4.8	Fox Islands, Aleutians			2		3
19 Apr 70	01:15:47.0	59.6N	142.7W	20	5.6	Gulf of Alaska			5		1
20 Apr 70	21:43:01.0	9.9S	119.2E	40	5.5	Sumba, Sunda Islands		1	6		1
22 Apr 70	11:38:01.9	11.4S	120.0E	33	5.6	South of Sumba, Sunda Islands			3	1	2
25 Apr 70	03:43:31.0	6.3S	69.8E	38	5.1	Chagos Archipelago			2	2	4
26 Apr 70	14:20:27.0	52.9N	171.5E	12	5.8	Near Islands, Aleutians			6		3
28 Apr 70	00:29:21.0	8.1S	156.4E	5	5.3	Solomon Islands			14		
28 Apr 70	01:12:17.4	8.1S	156.4E	24	5.5	Solomon Islands			14		
29 Apr 70	11:22:35.8	14.6N	92.8W	36	5.4	Coast Chiapas, Mexico			7	1	2
29 Apr 70	12:00:39.6	51.7S	177.0W	52	5.1	Rat Islands, Aleutians			3		3
29 Apr 70	18:01:29.7	55.5S	124.3W	33	5.7	Easter Island Cordillera		1	3	7	2
01 May 70	03:22:14.2	15.6N	121.8E	33	5.3	Luzon, Philippines	8			2	1
04 May 70	07:40:52.5	20.7S	173.5E	14	5.1	New Hebrides	5				6
04 May 70	18:53:21.0	41.7S	79.9E	33	5.4	Mid-Indian Ocean Rise				6	3
05 May 70	20:06:08.7	20.1S	170.2E	35	5.0	New Hebrides	4		7		8
06 May 70	02:35:17.5	15.7N	121.8E	41	5.1	Luzon, Philippines	5			2	1
06 May 70	15:21:55.0	9.8N	92.9E	32	5.3	Nicobar Islands	4		5		4
19 May 70	14:48:35.2	5.1S	152.3E	67	5.4	New Britain Island	6		9		2
20 May 70	20:03:35.0	55.9S	28.1W	6	6.1	South Sandwich Islands	3	1	18	4	2
20 May 70	20:30:54.7	51.4N	178.5W	47	5.6	Andreanof Islands	3		4		3
22 May 70	10:37:41.0	6.3S	154.7E	62	5.2	Solomon Islands	4		7		1
24 May 70	01:03:50.1	6.3S	154.5E	57	5.0	Solomon Islands	4		6		1
24 May 70	13:34:56.0	5.2S	152.0E	68	4.8	New Britain Island	5		4		1
25 May 70	16:47:36.0	29.6S	177.7W	65	5.4	Kermadec Islands	4		10	6	5

Date	Origin Time	Latitude	Longitude	Depth (km)	ISC m_b	Geographic Region	Number of Phase Readings obtained from each event				
							P	PD	PKP	PKP_1	PKP_2
29 May 70	05:14:42.0	15.0S	173.5W	70	5.4	Tonga Islands	5		6		8
29 May 70	10:33:58.7	24.0N	94.1E	49	5.1	Burma - India Border	7		10		
30 May 70	23:19:38.3	53.6N	164.2W	41	5.0	Unimak Island, Aleutians			2		3
31 May 70	20:23:28.4	9.2S	78.8W	48	6.4	Coast of Northern Peru	18	2	2	1	
01 Jun 70	01:36:10.1	9.3S	9.1W	45	5.9	Coast of Northern Peru			2		
01 Jun 70	02:45:18.8	10.2S	78.7W	43	5.8	Coast of Northern Peru	1		2		1
01 Jun 70	17:44:16.6	5.9N	82.6W	18	5.4	Central America	4		4		2
02 Jun 70	23:33:32.3	45.6N	151.0E	36	5.3	Kurile Islands			4	1	
04 Jun 70	04:09:25.4	9.9S	78.7W	48	5.8	Coast of Northern Peru	10	1	2	1	
05 Jun 70	04:53:07.4	42.5N	78.7E	24	5.9	Alma Ata, Kazakh, U.S.S.R.	10		2		1
05 Jun 70	07:00:42.5	38.5S	78.6E	33	4.9	Mid-Indian Ocean Rise				5	
05 Jun 70	13:54:44.5	52.1N	170.6W	46	4.8	Fox Islands, Aleutians			1		3
05 Jun 70	22:40:24.0	52.2N	159.5E	39	5.5	Coast of Kamchatka			6		1
06 Jun 70	06:14:13.3	62.8S	93.5W	33	4.8	South Pacific Ocean	1		1		4
07 Jun 70	04:12:08.0	40.3N	126.1W	13	4.7	Coast of Northern California					4
08 Jun 70	09:18:30.9	29.2S	61.1E	29	4.7	Atlantic-Indian Ocean Ridge				1	1
10 Jun 70	16:17:48.1	44.7N	149.5E	53	5.9	Kurile Islands	1		8		1
11 Jun 70	16:46:43.7	58.9S	157.6E	64	6.0	Macquarie Islands	6		7	7	3
12 Jun 70	08:06:17.0	2.9S	139.1E	32	5.9	Western New Guinea	7	3	5	1	1
13 Jun 70	05:27:54.7	51.6N	178.3W	55	5.5	Andreanof Islands	1		3		3
14 Jun 70	00:00:00.8	51.9S	74.1W	10	5.9	Coast of Southern Chile	8		12	1	
14 Jun 70	00:12:24.0	52.1S	74.3W	23	5.4	Coast of Southern Chile			5		
15 Jun 70	11:14:54.4	54.3S	64.2W	38	5.7	Falkland Islands	7	2	8	1	
17 Jun 70	00:48:11.7	6.0S	146.8E	49	4.8	Eastern New Guinea	1		3		1
19 Jun 70	10:56:13.5	22.3S	70.6W	44	6.1	Coast of Northern Peru	12		5	2	4

Date	Origin Time	Latitude	Longitude	Depth (km)	ISC m_b	Geographical Region	Number of Phase Readings obtained from each event				
							P	PD	PKP	PKP_1	PKP_2
21 Jun 70	16:11:49.0	9.5S	118.0E	22	5.2	Sumbawa, Sunda Islands			6	2	2
22 Jun 70	14:39:50.3	55.3N	156.4W	25	5.5	South of Alaska			2		5
23 Jun 70	03:38:36.4	60.8S	25.1W	40	5.3	Kurile Islands			5		
23 Jun 70	04:07:43.1	59.3S	159.4E	30	5.2	South Sandwich Islands			3	3	
25 Jun 70	05:13:59.0	7.9S	158.7E	70	5.9	Macquarie Islands	5		5	1	5
27 Jun 70	01:30:13.8	8.8S	124.0E	50	6.2	Solomon Islands	9	1	23		1
28 Jun 70	11:01:56.2	53.4N	160.3E	44	5.7	Timor, Sunda Islands	9	5	8	5	1
28 Jun 70	22:58:36.9	21.2S	174.3W	34	5.2	Coast of Kamchatka	1		7		
						Tonga Islands	2		4	1	9

APPENDIX II

Observatory, LRSM and NOAA Events (0-70 km)

Observatory, LRSM and NOAA Events (0-70 km)

Date	Origin Time	Latitude	Longitude	Depth (km)	NOS m_b	Recomputed m_b	Geographical Region	Observatory Observations P	PP	PD	PKP	PKP_1	PKP_2	LRSM Observations P	PP	PD	PKP	PKP_1	PKP_2	NOAA Observations P	PD	PKP	PKP_1	PKP_2
18 Jul 63	04:58:09.2	61.0S	22.3W	33	6.0		South Sandwich Islands		4	1	4													
30 Jul 63	13:51:57.8	55.9S	27.5W	33	6.2		South Sandwich Islands	1	3	1	3				2		5							
20 May 64	06:01:14.8	2.7S	139.3E	61	5.8		Western New Guinea	1	5	1	2			1	1		2							
25 May 64	19:44:07.0	9.1S	88.9E	33	5.5		Indian Ocean		2		1	4	4				2							
11 Jun 64	10:55:06.2	56.0S	27.3W	33	5.8		South Sandwich Islands		1		3								1		2			
13 Jun 64	08:23:45.6	10.0N	93.0E	33	6.1		Andaman Islands				4						1				1		1	
30 Jun 64	13:46:21.6	.8S	122.5E	36	6.3	6.0	Northern Celebes		5		5			1	2		3			3	4	1		
08 Jan 65	18:49:46.0	59.4S	24.0W	39	5.9		South Sandwich Islands		2		4						2		1		2			
09 Jan 65	13:32:46.4	11.9N	126.2E	5	6.1		Philippines	1	3	2	2			1	2	2	1			2				
12 Jan 65	13:32:24.0	27.6N	88.0E	23	6.1		Nepal	1	4		3			1	2	1	1				1			
24 Jan 65	00:11:12.1	2.4S	126.0E	6	6.6	6.0	Ceram Sea		S		3			1	2		6			2				
28 Jan 65	02:34:03.0	2.5S	102.5E	33	5.6		Sumatra		4		3		1	1	1		4				2			
11 Apr 65	00:11:08.8	42.7S	173.9E	7	6.2		South Island, New Zealand		4	1	2			2	2		2			1	1			
15 May 65	23:58:34.4	4.1S	135.1E	33	5.8	5.4	Western New Guinea		3	1	4			1			3			1				
16 May 65	11:35:46.0	5.3N	125.7E	36	6.2		Mindanao, Philippines	1	5		4			1			3			1	1		2	
17 May 65	17:19:25.9	22.5N	121.3E	21	6.2		Taiwan	3	5		2			5	8	1	2			2	2		1	
24 May 65	23:21:10.6	13.0N	124.5E	33	5.9		Samar, Philippines	1	4	1	2				2	1	2			1	1	2		
29 May 65	01:28:59.0	45.3S	95.9E	66	5.5		South Indian Ocean Rise					4	3					2	3			1		
31 May 65	11:38:28.0	7.5S	128.7E	37	6.0	5.7	Banda Sea		3		5			1	1		S			1	1	1		
03 Feb 66	11:58:35.3	16.6N	120.0E	69	5.8		Luzon, Philippines	1	1		1													
05 Feb 66	15:12:29.1	26.1N	103.1E	15	6.1	5.9	Yunan, China		4	1	3				3	2					1			
06 Feb 66	09:52:30.2	56.8S	25.4W	13	5.7		South Sandwich Islands		2		3				2		4		1					
07 Feb 66	04:26:13.9	29.8N	69.7E	33	6.0		West Pakistan		3	1	3				1		2			1	1			
07 Feb 66	05:21:44.6	30.0N	69.9E	10	5.4	5.3	West Pakistan		1		2						1				1			
07 Feb 66	23:06:34.5	30.2N	69.8E	10	5.8		West Pakistan		4	2	3				2		1							
09 Feb 66	07:18:47.8	9.9S	116.3E	32	5.8		Sumbawa Island		1		3	1	1		1		6	1	1					
13 Feb 66	06:35:55.7	6.6S	132.6E	12	5.9	5.8	Tanimbar Island		2	1	4						4			3	3		1	
13 Feb 66	10:44:41.0	26.1N	103.2E	33	5.7		Yunan, China		2		2				2						1			
17 Feb 66	11:48:00.8	32.2S	78.9E	33	6.4		Mid-Indian Ocean Rise		3			5	5		5		1	4	5			2	2	
17 Feb 66	12:43:01.1	32.2S	79.0E	33	5.7		Mid-Indian Ocean Rise		5			5	5		1		1	5	7			2	1	1
21 Feb 66	00:22:29.5	55.7S	26.9W	33	5.9		South Sandwich Islands	1	4	1	3				1		6					4	1	1
22 Feb 66	05:02:37.2	5.4S	151.5E	28	6.2		New Britain Island	3	3	1	1					1	3							
14 Sep 66	23:18:41.6	60.2S	27.2W	22	6.2	5.9	South Sandwich Islands		3	1	4			1	4		5			1				
15 Sep 66	11:51:55.7	60.3S	26.7W	33	5.7		South Sandwich Islands		1		3													
18 Sep 66	20:43:53.3	27.8N	54.3E	16	6.2		Southern Iran		I	2	1				1	1	2							1
28 Sep 66	14:00:22.9	27.4N	100.1E	33	6.2		Yunan, China		4	1	2				3	I	1							
19 Mar 67	01:10:45.8	6.7S	129.9E	60	5.9		Banda Sea		3		5			2	7		7			3	1	9		3
22 Aug 67	13:02:06.8	60.8S	24.6W	33	6.1		South Sandwich Islands		2		4				7		8		2	1		2	2	2
22 Aug 67	13:17:02.5	60.9S	23.2W	19	5.9	5.7	South Sandwich Islands		2		3				I		6		2			2		5
12 Oct 67	18:31:37.1	7.1S	129.8E	45	6.2		Banda Sea		2		4			2	1		1			7		9		
10 Aug 68	02:07:04.3	1.4N	126.2E	33	6.3		Mulucca Passage		2	1	3												1	1
10 Aug 68	05:51:47.9	1.5N	126.2E	33	6.2		Molucca Passage		3	I	3									5		1	4	1
10 Aug 68	08:10:16.3	1.6N	126.2E	33	5.6		Molucca Passage		2	1	3									2		2	2	
11 Aug 68	20:00:43.4	1.6N	126.1E	33	5.9		Molucca Passage		3	1	3									1			2	1
31 Oct 68	09:06:36.4	1.2N	126.3E	33	6.1		Molucca Passage		1	1	3									7	2	4		